Effets de la force de Coriolis sur l'instabilité elliptique en géométries cylindrique et sphérique

Michael Le Bars, Stéphane Le Dizès, & Patrice Le Gal

IRPHE - CNRS UMR 6594, 49 rue F. Joliot Curie, B.P. 146, F-13384 Marseille Cedex 13
lebars@irphe.univ-mrs.fr

Résumé. Nous avons étudié expérimentalement les effets de la force de Coriolis sur l'instabilité elliptique dans des cylindres et des sphères mis en rotation et embarqués sur une table tournante. Différents modes instables peuvent être excités en ajustant le rapport Ω^G entre la rotation globale de la table et la rotation du fluide, en accord avec la théorie globale de l'instabilité elliptique. Aucune instabilité n'est présente pour $-3/2 < \Omega^G < -1/2$. En diminuant Ω^G progressivement vers $-1/2$, nous observons différentes bandes de résonance, tout d'abord discrètes, puis se superposant. Simultanément, les taux de croissance et nombre d'onde du mode le plus instable augmentent significativement, en accord quantitatif avec la théorie locale. En géométrie sphérique, de nouvelles résonances ont été observées pour la première fois, en complément du mode classique de "spin-over". Ces résultats ont des implications significatives dans des contextes astro- et géophysiques.

Abstract. The effects of Coriolis force on the elliptical instability are studied experimentally in cylindrical and spherical rotating containers embarked on a table rotating at a fixed rate. For a given set-up, changing the ratio Ω^G of global rotation to flow rotation leads to the selection of various unstable modes due to the presence of resonance bands, in close agreement with the normal mode theory. No instability takes place when Ω^G ranges between -3/2 and -1/2 typically. When decreasing Ω^G toward -1/2, resonance bands are first discretized for $\Omega^G > 0$ and progressively overlap for $-1/2 < \Omega^G < 0$. Simultaneously, the growth rates and wavenumbers of the prevalent stationary unstable mode significantly increase, in quantitative agreement with the viscous short-wavelength analysis. New complex resonances have been observed for the first time in the sphere, in addition to the standard spin-over. We argue that these results have significant implications in geo- and astrophysical contexts.

1 Introduction

The elliptical instability corresponds to the three-dimensional destabilisation of two-dimensional rotating flows with elliptical streamlines (see the review by Kerswell [7] and references therein). It has first been discovered in the context of strained vortices, but it generally appears in any turbulent flow exhibiting some coherent structures with elliptical motion as well as in a large range of industrial and natural systems (e.g. in the wake vortices behind aircrafts, in planetary liquid cores, in binary stars and accretion disks), where the ellipticity is generated either by vortex interactions or by tidal effects.

In most practical cases, the strain field responsible for the elliptical pattern rotates around the same axis as the flow, but with a different rate and possibly in an opposite direction. In the present paper, we thus systematically study the effects of Coriolis force on the elliptical instability, both in a rotating cylinder and in a rotating spheroid. Our experimental set-up is inspired from Malkus [14] : it is similar to the one already used in [4] and [11] respectively. Contrary to former devices, it permits to analyse the growth and the saturation of the elliptical instability. A deformable and transparent container - either a cylinder of radius $\tilde{R} = 2.75$cm and height $\tilde{H} = 21.4$cm or a hollow sphere of radius $\tilde{R} = 2.175$cm - is set in rotation about its axis (Oz) with an angular velocity $\tilde{\Omega}^F$ up to 300rpm and is simultaneously deformed elliptically by two fixed rollers parallel to (Oz). The container is filled with water seeded with anisotropic particles (Kalliroscope). A light sheet is formed in a plane containing the rotation axis for visualisation, allowing the measurement of wavelengths and frequencies of excited modes. Besides, the whole set-up (with also the camera and light projector) is placed on a 0.5m-diameter rotating table, which allows rotation with angular velocity $\tilde{\Omega}^G$ up to $\pm$60rpm. Our protocol is the same all along the

experiments presented here. First, we set the global rotation to its assigned value and wait for solid body rotation to take place in the container. Then we start the rotation of the container : a spin–up phase first takes place, before the possible development of an instability. All presented experiments are carried out near the instability threshold : the characteristic growth time is then much larger than the spin–up time and decorrelation of both phenomena is expected.

2 Theoretical and experimental study in the cylinder

2.1 Theoretical approaches

The elliptical instability mechanism has been reviewed in [7]. It is associated with the parametric resonance of two inertial waves of the undistorted circular flow induced by the underlying strain field (e.g. [17,7]). For small deformations, the global (or normal mode) theory permits to calculate explicitly the conditions of resonance for a given geometry and provides information on the structure of the eigenmodes. Results for the elliptical instability in a cylinder with Coriolis effects have been obtained by Kerswell [6]. Numerous resonances with various structures can be excited by changing the global rotation rate $\Omega^G = \tilde{\Omega}^G/\tilde{\Omega}^F$ only, except in a forbidden band for Ω^G between $-3/2$ and $-1/2$ where the elliptical instability cannot develop.

In addition to the conditions for resonance given by the global approach, the local approach allows the analytical determination of the growth rate of the instability. It is based on the inviscid short–wavelength Lagrangian theory [2,3]. In this approach, perturbations are assumed to be sufficiently localised in order to be advected along flow trajectories and are searched in the form of local plane waves. This method has been applied to the elliptical instability with global rotation by Le Dizès [13]. He determined the exponential growth rate at order 1 in eccentricity ε

$$\sigma = \sqrt{\left(\frac{3+2\Omega^G}{4(1+\Omega^G)}\right)^4 \varepsilon^2 - \left(1-2|1+\Omega^G|\cos(a)\right)^2}, \tag{1}$$

where a is the angle between the flow rotation axis and the wavevector.

Assuming that the viscous dissipation is of order ε, viscous effects on the localised perturbations can be easily taken into account by adding the viscous damping rate $-k^2\mathrm{Re}^{-1}$ [3]. Here Re is the Reynolds number defined by $\mathrm{Re} = \tilde{\Omega}^F\tilde{R}^2/\nu$, ν the kinematic viscosity of the fluid and k the wavevector of the perturbation. Viscous effects on the surface of the container for plane wave perturbations can be estimated using the work of Kudlick [9] and introduce corrections of order $\mathrm{Re}^{-1/2}$. For given values of $(\tilde{R}, \tilde{H}, \tilde{\Omega}^F, \nu, \varepsilon)$, bands of instability then take place depending on the global rotation rate Ω^G , each band corresponding to a given axial structure determined by the number n of axial half-periods. Two examples of these theoretical predictions are shown in figure 1, together with our experimental data.

2.2 Experimental study

A series of experiments was performed using a cylinder of height $\tilde{H} = 21.4$cm and eccentricity $\varepsilon = 0.085$, systematically changing $\tilde{\Omega}^F$ and $\tilde{\Omega}^G$. Good agreement is found with the linear inviscid global approach : stationary mode with a sinusoidal rotation axis and various wavelengths (figure 2) as well as other more exotic modes recognised by their complex radial structure and/or by their periodic behaviour can be selected by changing the dimensionless ratio Ω^G only, providing the Reynolds number is large enough.

The growth rate of the stationary mode can be determined experimentally : from sequences of images, we measure the maximum amplitude of the sinusoidally deformed rotation axis ; its temporal evolution is then fitted with an exponential growth, which can be compared to the exponential growth rate determined by the local theory (see figure 1). First, one can notice that the threshold for instability agrees with the theory, with for instance the sharp disappearance of resonant modes at $\Omega^G_c = -0.520 \pm 0.004$ for $\tilde{\Omega}^F = 0.505 \pm 0.005$Hz. Besides, measurements of the growth rate qualitatively agree with the theory, regarding

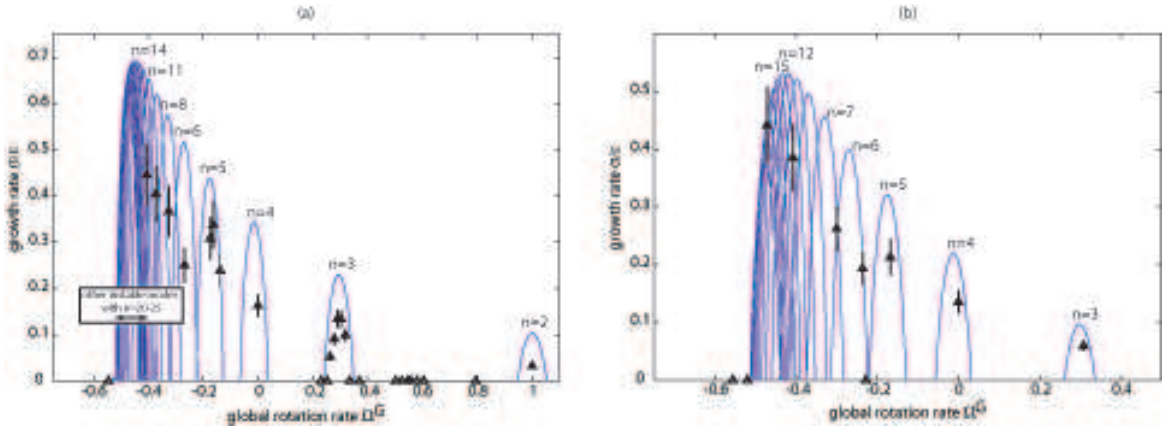

Fig.1. Viscous growth rate of the elliptical instability determined by the local analysis as a function of the global rotation rate Ω^G for a given cylinder of radius $\tilde{R} = 2.75$cm, height $\tilde{H} = 21.4$cm, eccentricity $\varepsilon = 0.085$, filled with water ($\nu = 10^{-6} m^2 s^{-1}$) : (a) $\tilde{\Omega}^F = 0.505 \pm 0.005$Hz ($\mathrm{Re} = 2.40 \times 10^3$) and (b) $\tilde{\Omega}^F = 0.255 \pm 0.002$Hz ($\mathrm{Re} = 1.21 \times 10^3$). Triangles stand for experimental measurements and solid lines for theoretical predictions. The predicted number n of axial half-wavelengths increases by 1 from the right to the left on each resonant band, starting from $n = 2$ in (a) and $n = 3$ in (b) ; measured values are indicated above each experimental point. Note that in (a), additional resonances were observed for Ω^G in the range $[-0.507; -0.403]$; nevertheless, because of their small wavelength and their rapid growth rate, quantitative measurements were not accurate.

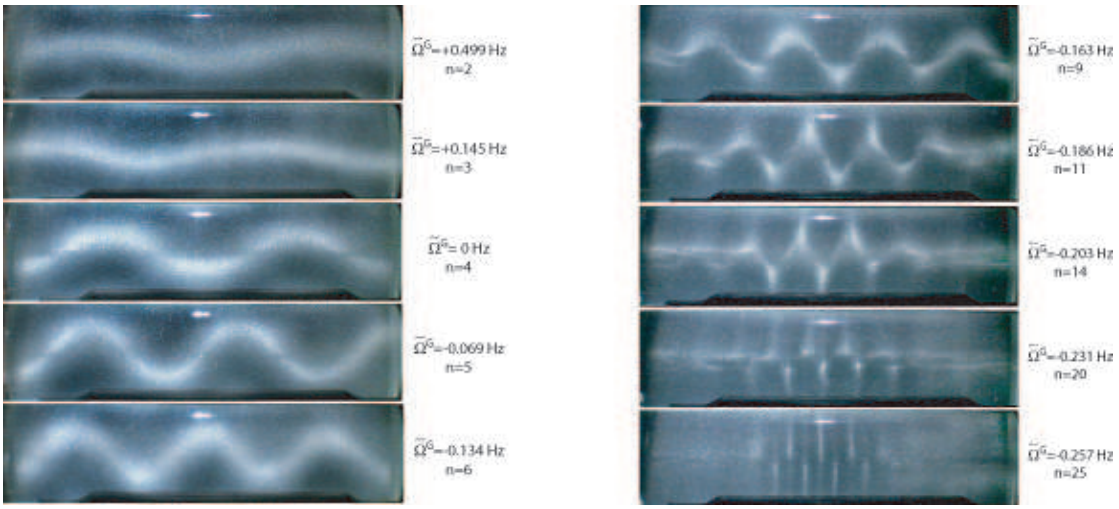

Fig.2. Variation of the wavelength of the elliptical instability versus the global rotation $\tilde{\Omega}^G$ for a given cylinder of radius $\tilde{R} = 2.75$cm and height $\tilde{H} = 21.4$cm with an eccentricity $\varepsilon = 0.085$ rotating at $\tilde{\Omega}^F = 0.505 \pm 0.005$Hz ($\mathrm{Re} = 2.40 \times 10^3$). In these pictures, the rotation axis is horizontal.

the general increasing trend when Ω^G decreases toward $-1/2$, and also regarding the specific shape of one resonance band (see for instance in figure 1*a* the band around $\Omega^G = 0.285$ that we have explored in detail). Quantitatively, orders of magnitude also agree, but theoretical values always overestimate experimental values. Three main explanations can be provided. First, non-linear effects were not taken into account in the theory, but are expected to be stabilising [4]. Then, it is worth recalling that the theoretical estimate is based on a short–wavelength (i.e. large k) asymptotic analysis : the discrepancy could therefore be associated with finite k effects. The last source of discrepancy is experimental, since in our set-up, rollers only deform the central part of the cylinder.

3 Theoretical and experimental study in the sphere

The eigenmodes of the sphere have been studied in the non-rotating case by Greenspan [5]. His study can be modified to take into account an additional Coriolis force, similarly to what has been done for the cylindrical case. The global rotation leads to exactly the same changes as in the cylinder. Hence, in contrast with the non-rotating case where the only exact resonance in the sphere leads to the spin–over mode (i.e. a solid body rotation around the axis of maximum strain, see [11]), the analytical study suggests that more complex instabilities can be triggered by the global rotation.

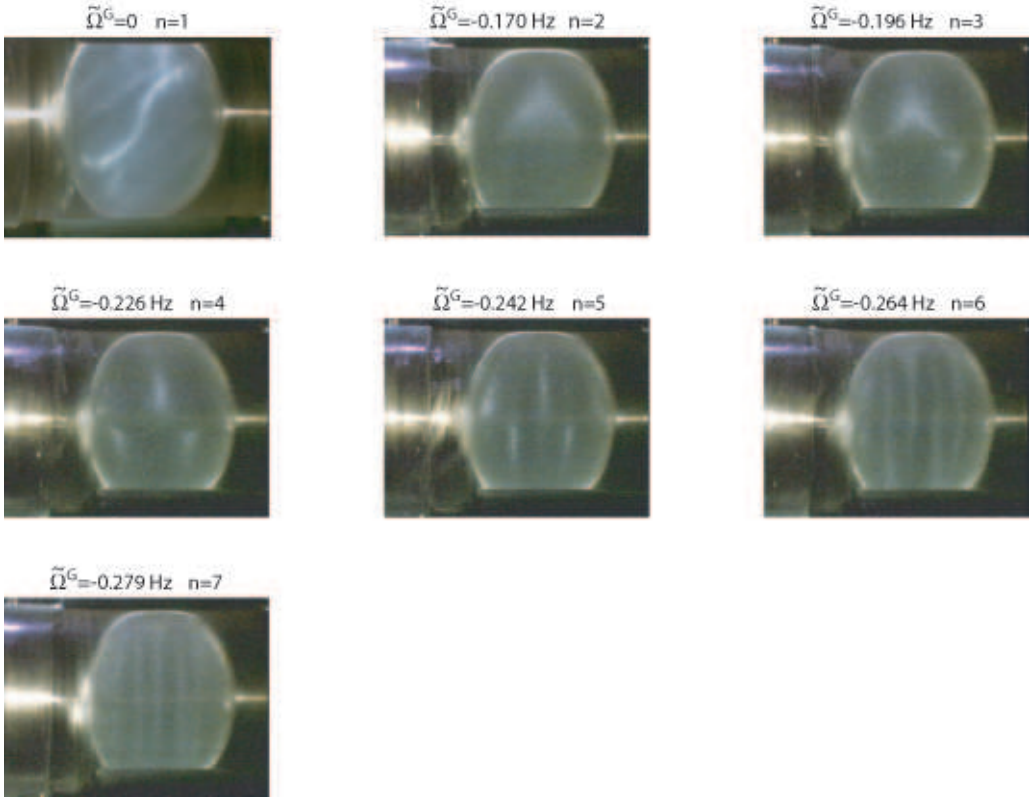

Fig.3. Pictures of the flow structure associated with the elliptical instability for different global rotation rates $\tilde{\Omega}^G$ in the deformed sphere with an eccentricity $\varepsilon = 0.20$ and a fixed fluid rotation $\tilde{\Omega}^F = 0.500 \pm 0.005$Hz (Re $= 1.49 \times 10^3$). The measured number n of axial half-wavelengths is also indicated. In these pictures, the rotation axis is horizontal.

A series of experiments was performed in the sphere of radius $\tilde{R} = 2.175$cm with a fixed eccentricity $\varepsilon = 0.20$, systematically changing $\tilde{\Omega}^G$ and $\tilde{\Omega}^F$ to excite various resonances. In the explored range $-0.6 < \Omega^G < 0$, we observed the same behaviour as in the cylinder : when Ω^G decreases towards $-1/2$, the number of axial structures as well as the growth rate of the instability rapidly increase (see figure 3), until the instability suddenly disappears in the vicinity of $\Omega^G \sim -1/2$. Excited modes are in good agreement with analytical predictions for Ω^G ranging in a resonance band of ± 0.03 typically around the theoretical perfect–resonance value. With our experimental device, the visualisation in the sphere was not precise enough to allow a systematic measurement of the growth rate of the elliptical instability, but we determined experimentally the viscous threshold of instability for two given values of the flow rotation rate : $\Omega_c^G = -0.557 \pm 0.004$ for $\tilde{\Omega}^F = 0.501 \pm 0.005$Hz and $\Omega_c^G = -0.551 \pm 0.004$ for $\tilde{\Omega}^F = 0.747 \pm 0.005$Hz. We recall that in the absence of global rotation, the only perfect resonance and the only observed mode

in the vicinity of threshold (i.e. at low Reynolds number) is the spin-over, corresponding to a single additional rotation around the axis of maximum strain [11].

4 Conclusion

In this paper, we have presented the analytical and experimental study of the influence of Coriolis force on the elliptical instability. For a given container - either cylindrical with a fixed aspect ratio $\tilde{H}/\tilde{R}$ or spherical -, the global rotation rate allows to select various resonances, in good agreement with the global theory. In particular, we have observed in the sphere numerous complex stationary modes at relatively low values of the Reynolds number, in addition to the simple spin-over that takes place in the non–rotating case. For both the cylinder and the sphere, when decreasing progressively the global rotation rate, we have observed that various bands of resonance coexist for $\Omega^G \geq \Omega_c^G \sim -1/2$, first separated by large regions of stability (especially for cyclones), then progressively overlapping (especially for anticyclones). All resonances sharply disappear once the global rotation rate reaches a critical value $\Omega_c^G \sim -1/2$. Focusing on the stationary modes, we have shown that the instability wavenumber as well as its growth rate significantly increase and reach a maximum just before Ω_c^G. In the cylindrical geometry, all these results agree quantitatively with the theoretical estimations taking into account the viscous corrections. Our conclusions in the cylinder and in the sphere also agree qualitatively with the general trend observed by Afanasyev [1] in vortex pairs and by Stegner et al. [16] in Karman vortex streets, even if our experimental set-up is totally different (i.e. their vortices are not confined and are subjected to rather large elliptical deformations). Indeed, both studies report the systematic destruction of elliptical anticyclones by a sinusoidal mode with a decreasing wavelength when Ω^G decreases up to a certain critical value, corresponding to the overlapping resonances mentioned here. We thus argue that this behaviour is universal, except for the explicit value of Ω_c^G that will depend both on the considered vortical structure and on the value of the eccentricity (see also [15,13]).

Conclusions in the spherical geometry are especially interesting in the geophysical and astrophysical contexts. For instance, complex motions can be expected in the Earth's core in addition to the simple spin-over excited by both precession and elliptical instability. More generally, one can imagine that binary stars and moon–planet systems where the elliptical instability is expected to take place, encounter various bands of instability during their evolution : depending on the relative changes in their rotation and revolution rates, different and complex histories regarding energy dissipation and flow motions can thus be expected. Clearly, the role of the elliptical instability in natural flows [8] still demands more works, in order to fully understand the implications of all natural complexities on the standard and well-known hydrodynamical model (see also [10,12]).

Références

1. Y. D. Afanasyev, Experiments on instability of columnar vortex pairs in rotating fluid, *Geophys. Astrophys. Fluid Dyn.* **96(1)**, 31–48 (2002).
2. B. J. Bayly, Three-dimensional instability of elliptical flow, *Phys. Rev. Lett.*, **57**, 2160–63 (1986).
3. A. D. D. Craik & W. O. Criminale, Evolution of wavelike disturbances in shear flows — a class of exact solutions of the Navier-Stokes equations, *Proc. Roy. Soc.* **A406**, 13–26 (1986).
4. C. Eloy, P. Le Gal & S. Le Dizès, Elliptic and triangular instabilities in rotating cylinders, *J. Fluid Mech.* **476**, 357–388 (2003).
5. H. P. Greenspan, *The theory of rotating fluids*. Cambridge University Press (1968).
6. R. R. Kerswell, Tidal excitation of hydromagnetic waves and their damping in the Earth. *J. Fluid Mech.* **274**, 219–41 (1994).
7. R. R. Kerswell, Elliptical instability, *Annual Review of Fluid Mechanics*, **34**, 83–113 (2002).
8. R. R. Kerswell & W. V. R. Malkus, Tidal instability as the source for Io's magnetic signature, *Geophys. Res. Lett.* **25**, 603–6 (1998).

9. M. Kudlick, *On the transient motions in a contained rotating fluid*, PhD thesis, MIT (1966).
10. L. Lacaze, W. Herreman, M. Le Bars, S. Le Dizès & P. Le Gal, Magnetic field induced by elliptical instability in a rotating spheroid, *Geophys. Astrophys. Fluid Dyn.*, **100**, 299–317 (2006).
11. L. Lacaze, P. Le Gal & S. Le Dizès, Elliptical instability in a rotating spheroid, *J. Fluid Mech.*, **505**, 1–22 (2004).
12. M. Le Bars & S. Le Dizès, Thermo-elliptical instability in a rotating cylindrical shell, *J. Fluid Mech.*, **563**, 189–198 (2006).
13. S. Le Dizès, Three-dimensional instability of a multipolar vortex in a rotating flow, *Phys. Fluids* **12**, 2762–74 (2000).
14. W. V. R. Malkus, An experimental study of the global instabilities due to the tidal (elliptical) distortion of a rotating elastic cylinder, *Geophys. Astrophys. Fluid Dyn.*, **48**, 123–34 (1989).
15. D. Sipp, E. Lauga & L. Jacquin, Vortices in rotating systems : centrifugal, elliptic and hyperbolic type instabilities, *Phys. Fluids*, **11**, 3716–28 (1999).
16. A. Stegner, T. Pichon & M. Beunier, Elliptical-inertial instability of rotating Karman streets, *Phys. Fluids*, **17**, 066602 (2005).
17. F. A. Waleffe, On the three-dimensional instability of strained vortices, *Phys. Fluids*, **2**, 76–80 (1990).